FINITE ELEMENT SIMULATION OF ION CURRENTS FROM CORONATING HVDC OVERHEAD LINES

U. Straumann[1*] and C. M. Franck[1]
[1]High Voltage Laboratory, ETH Zurich, Physikstrasse 3, 8092 Zürich, Switzerland
*Email: stulrich@ethz.ch

Abstract: Today's need for transmission capacity is continuously growing. As it is difficult to obtain new rights-of-way, options such as replacing existing AC- by DC-lines to maximize the power capability of existing corridors are required.
So as to limit land use, overhead transmission lines have been built as multi-circuit AC-lines on the same structure in many countries. Changing one AC circuit to DC results in transmission lines with AC/DC hybrid towers in such situations. With practically no hybrid AC/DC-line realized worldwide so far, questions concerning the mutual interaction of the different circuits arise, such as superimposed AC- and DC-fields intensified with corona-generated space-charges.
In contrast to such hybrid lines, the problem of calculating the ion flow fields of HVDC-lines has been widely addressed in literature; undoubtedly it can be numerically solved very precisely. However, great uncertainty exists about the boundary conditions, i.e. the amount of ions produced by corona.
In the work presented here, the numerical calculation of ion-currents and electric fields of DC-lines by means of a finite-element-method software is reproduced. The novelty is the time-dependence of the simulation, needed for the case of hybrid lines, and boundary conditions yielding results in closer accordance with experimental data found in literature.

1 INTRODUCTION

As in the case of AC, corona is an important phenomenon to be considered when planning DC high voltage overhead transmission lines. However, there are differences between the impact of AC and DC corona and their dependence on environmental parameters.

For example, the increase of corona activity from fair to foul weather is smaller in the case of DC than AC. One reason for this is that DC-lines are more prone to coronating pollution, as particles or insects, once charged, are attracted continuously to the corresponding poles [1] (section 3). Therefore, DC-corona depends on the weather as well as on the climate. Further, due to triboelectricity, pollution of the positive pole is more intense, leading to increased corona activity on this pole [1] (section 3).

The effects of the space-charge due to corona-generated ions from HVDC lines are manifold, such as [1] (section 1)

- corona loss
- enhanced electric fields on grounded objects, which increases the risk of corona on grounded objects
- ion current onto ground (as DC current), resulting in effects such as charging of objects

However, currents are small (smaller than in the case of AC) and ions do not seem to be harmful to human or animal health [1] (section 4). Nevertheless, ion density and current as well as the electric field on the ground are considered to be important aspects of HVDC lines; ions are seen as potentially the most severe constraint when planning DC-lines [1] (section 1).

Therefore, first short-term fair weather measurements such as shown in [2] investigated these environmental impact quantities, i.e. electric fields on ground, ion currents onto and charge densities on ground under HVDC lines. Such data for long term measurements and for different weather conditions became available with [3].

According to [4], the ion flow problem without simplification with Deutsch's assumption (after which space charges alter only the magnitude but not the direction of the electric field) was for the first time solved by means of the finite element method (FEM) by [5]. Other methods to compute the ion flow problem are applicable as well, as for example the charge simulation method [6].

With the upwind FEM Takuma et al. [4] introduced a technique to prevent numerical instabilities and accounted for the presence of wind changing the ion flow field. The former is of special importance, as the set of equations governing the ion flow field contain diffusion-less transport equations, which are especially prone to numerical instabilities. After [4], further works on the ion flow field of HVDC-lines used the upwind method, such as [7] and [8].

However, some advocate the use of more powerful techniques such as the streamline upwind Petrov-Galerkin FEM (SUPG) [9], where using this method improves the quality of numerical results, i.e. these match the experimental data better. However, it seems to be questionable whether the lack of strong numeric methods or merely the lack of accurate boundary conditions reflecting the coronating conductors is responsible for the better part of the difference between the numerical and experimental results in literature. Especially the asymmetry of corona activity during fair weather periods between positive and negative poles due to different pollution of the conductors can only be assessed by different boundary conditions for the two polarities. However, the widely used condition is surface gradients fixed at the corona onset values such as in [4, 5, 7, 8, 10] and [11].

The novelty in this paper is the time-dependent formulation and implementation of the ion flow field problem. Even though it is adapted to the stationary problem of a HVDC line here, it permits future investigations of time-dependent problems, such as AC/DC hybrid lines. Further, other boundary conditions from literature describing the ion generation are used.

2 BIPOLAR ION FLOW FIELD EQUATIONS

The problem is restricted to simple 2d-geometries in flat open country. The line is described by the conductors, which are represented with a circle per subconductor. Obviously, the size of the space around the line has to be restricted to a finite domain, by adding artificial boundaries of the domain laterally and above (referred to as *"outer boundaries"* in the following), see Figure 1.

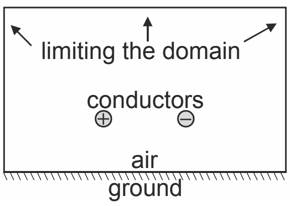

Figure 1: Domain and boundaries

2.1 Basic Equations

In the domain constituted by the air encircled by the "*outer boundaries*", ground and the conductors (Figure 1), the unknowns, i.e. space-charge densities ρ^+ and ρ^- of positive and negative ions respectively and the potential ϕ have to be determined.

For these quantities, Poisson's equation reads

$$\Delta\phi = -\left(\rho^+ - \rho^-\right)/\varepsilon_o . \quad (1)$$

The continuity equations for the two space-charge densities $\rho^\pm$ (the two algebraic signs correspond to the related polarity) are

$$-\partial_t \rho^\pm - r\rho^+\rho^- = \operatorname{div} \mathbf{j}^\pm, \quad (2)$$

where r equals the recombination coefficient R divided by the elementary charge e. The current density $\mathbf{j}$ is given by the drift of the ions (neglecting diffusion)

$$\mathbf{j}^\pm = \rho^\pm \cdot \mathbf{v}^\pm = \mp\mu^\pm\rho^\pm \cdot \nabla\phi, \quad (3)$$

with μ as the mobility of the ions.

Insertion of (3) in (2) and using (1) leads (with the assumption of constant ion mobility) to

$$-\partial_t \rho^\pm - r\rho^+\rho^- \mp \frac{\mu^\pm}{\varepsilon_o} \cdot \rho^\pm\left(\rho^+ - \rho^-\right) \pm \mu^\pm\left(\nabla\rho^\pm\right)\nabla\phi = 0. \quad (4)$$

These three equations (1) and (4) govern the ion flow field in the domain.

2.2 Boundary Conditions

In the following the boundary conditions are discussed.

2.2.1 Electric potential The boundary condition of the potential on ground and conductors are obviously given by the corresponding potentials.

In the case of the "*outer boundaries*", reality is approximated by a symmetry condition, i.e.

$$\mathbf{n} \cdot \nabla\phi = 0, \quad (5)$$

with the unit normal vector $\mathbf{n}$.

2.2.2 Ion densities Even though because of (5), the ion densities are zero on the "*outer boundaries*", non-reflecting boundary conditions are implemented on all boundaries: Ions drifting onto the boundary are absorbed. If the upwind element to a corresponding ion density at the boundary does not exist, the ion density is set to zero or to the corresponding density, in case of coronating conductors.

2.2.3 Ion production on coronating conductors The typical boundary condition by determining a corona onset-field strength which is not surmounted due to shielding by the produced ions has the drawback that especially in the case of only few protrusions (e.g. fair weather), this onset field strength value is not applicable everywhere on the conductor. Then only some local parts of the conductor are under corona. This is why the concept of saturation of [1] (section 3 and 4) is quite convincing.

In [1] (section 3), the saturated ion current from the single poles I_{bs} is defined as the theoretical limit current leading to a complete shielding of the conductor from the field due to the space charges (i.e. the voltage on the conductor due to space charges already reaches the conductor potential).

Then the effective corona current $I_{\mathrm{c}}^{\pm}$ is according to [1] (section 3) given by

$$I_{\mathrm{c}}^{\pm} = S^{\pm} \cdot I_{\mathrm{bs}}^{\pm}, \tag{6}$$

with $S^{\pm}$ as corona saturation

$$S^{\pm} = 1 - \exp[-k^{\pm}\left(E - E_o^{\pm}\right)], \tag{7}$$

E as prospective (corona-free) average surface gradient of the conductor and $E_o^{\pm}$ and $k^{\pm}$ as constants, which depend on the climate.

For bipolar lines the saturated corona current is according to [1] (section 3 and 4)

$$I_{\mathrm{bs}}^{\pm} = K^{\pm} \cdot 6.16 \cdot 10^{-15} \cdot \left(\left(V^{+} - V^{-}\right)/2\right)^{2} \Big/ \left(F^{\pm} \cdot P\right)^{2}, \tag{8}$$

if the pole spacing is much smaller than the height above ground (neglecting the monopolar component, which is only an approximation here), with

$$K^{\pm} = \begin{cases} 1 & \text{for } + \\ 1.3 & \text{else} \end{cases}, \quad F^{\pm} = \begin{cases} 0.467 & \text{for } + \\ 0.533 & \text{else} \end{cases},$$

V_1 and V_2 the voltages applied to the conductors 1 and 2 and P as the distance between the poles. Obviously, this is an empiric way to determine the corona current I_{c}.

Unlike in [1], the actual E is used here to implement a back coupling of the space charges on the local corona activity. This prevents unphysically excessive corona. The choice of the local value of the surface gradient also respects the circumstance that the corona activity is not constant along the conductor contours, because the surface gradients are not constant (the surface gradients on subconductors are smaller on the side near to the other subconductors than on the outer side of the bundle).

This procedure is adopted as boundary condition as follows: The current density is calculated according to

$$i^{\pm} = I_{\mathrm{c}}^{\pm} / A, \tag{9}$$

with A as the sum of the circumference of all subconductors of the bundle. The boundary condition for the ion densities on the conductors is therefore given by

$$\rho^{\pm} = i^{\pm} \Big/ \left(\mu^{\pm} E\right). \tag{10}$$

3 IMPLEMENTATION

The problem is implemented in a common FEM-software. To overcome numerical instability, the widely used upwind method is adopted.

3.1 Validation Case

As some previous works such as [8, 9] and [11] used measurement results of [3] as benchmarks for the calculation methods, such cases will be investigated here as well. The geometry of the line is sketched in Figure 2. It consists of one ±400 kV bipole, equipped with a two-conductor bundle, of which the subconductor diameter is 3.82 cm and their separation 45.7 cm.

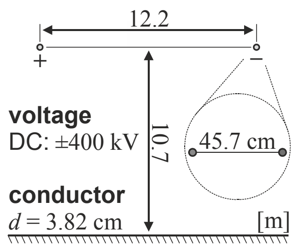

Figure 2: Investigated geometry, data from [3]

In the first second the system is energised with a linear ramp to nominal voltage. To reach asymptotically stationary conditions, the evolvement of the ion flow field is calculated for additional 49 s after reaching nominal voltage. As no relevant change of the quantities is observed already after the first ten seconds, the results after 50 s are felt to be a good approximation of the stationary case.

3.2 Parameters

The mobilities $\mu^{\pm}$ and the recombination coefficient R is chosen as

$$\begin{aligned} \mu^{+} &= 1.2 \cdot 10^{-4} \ \ \mathrm{m}^2/\mathrm{Vs} \\ \mu^{-} &= 1.5 \cdot 10^{-4} \ \ \mathrm{m}^2/\mathrm{Vs} \end{aligned} \tag{11}$$

and

$$R = 1.8 \cdot 10^{-12}, \tag{12}$$

respectively. The size of the "*outer boundary*" is 60 m in height and 120 m in width.

3.2.1 Fair weather corona current parameters The parameter $E_o^{\pm}$, $k^{\pm}$ determining the saturation S are

50% values (i.e. reached over 50% of the time, as are the measurement data from [3] taken for comparison), reading

$$E_o^+ = E_o^- = 14.5 \text{ kV/cm}, \quad k^+ = 0.041, \quad k^- = 0.021, \tag{13}$$

according to [1] (section 4) for spring fair weather conditions. The arbitrary choice of spring fair weather parameters lead to a better match with the experimental results than the summer fair weather parameters, where calculated corona activity becomes too large.

3.2.2 Foul weather corona current parameters
The same 50% values for foul weather are according to [1] (section 4)

$$E_o^+ = E_o^- = 6 \text{ kV/cm}, \quad k^+ = k^- = 0.058. \tag{14}$$

4 RESULTS

4.1 Ion Distribution

Qualitative impressions of the calculation results for the case of spring fair weather are shown in Figure 3 and Figure 4 for the total space-charge density $\rho = \rho^+ - \rho^-$ and the product of the space-charge densities $\rho^+ \cdot \rho^-$ respectively. The latter is proportional to the recombination rate. Also visible in these figures are the equipotential lines.

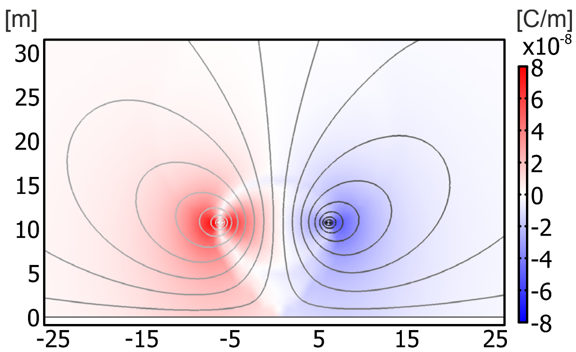

Figure 3: Fair weather total charge density distribution and equipotential lines; red color corresponds to positive (max. 80 nC/m^3), blue to negative (min. -52 nC/m^3) charge

Figures 3 and 4 clearly show the effect of non-homogeneous ion production over the subconductor contours.

While positive ions are produced in greater numbers, negative ions inherit a higher mobility. Most probably, the latter is responsible for the higher densities of negative ions slightly visible in the areas with low ion densities between the two poles.

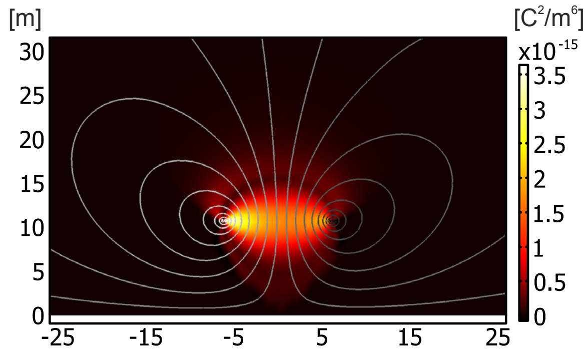

Figure 4: Fair weather ion densities product distribution and equipotential lines

Figure 4 indicates that space-charges are more numerous near the positive pole due to the above-mentioned asymmetry of the ion current parameters respecting the more severe corona on the positive pole during fair weather and the higher mobility of negative ions.

4.2 Electric Fields on Ground

The resulting electric surface gradients on ground are depicted in Figure 5 and Figure 6 for fair and foul weather respectively.

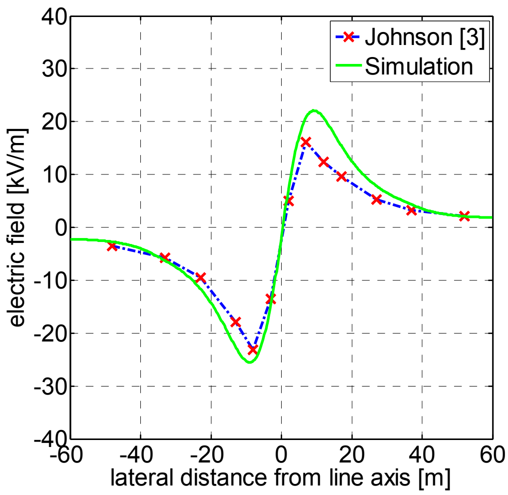

Figure 5: Fair weather electric field under the line

Practically all calculated values are larger than the measured ones. Nevertheless, they match the experimental data fairly well.

While the experiment shows a relevant asymmetry between negative and positive extrema (i.e. a deviance when mirroring the curve at the origin) for fair weather, practically none is present in foul weather. The same is true for the calculated results; however, the calculated asymmetry during fair weather is too small compared to the measured one.

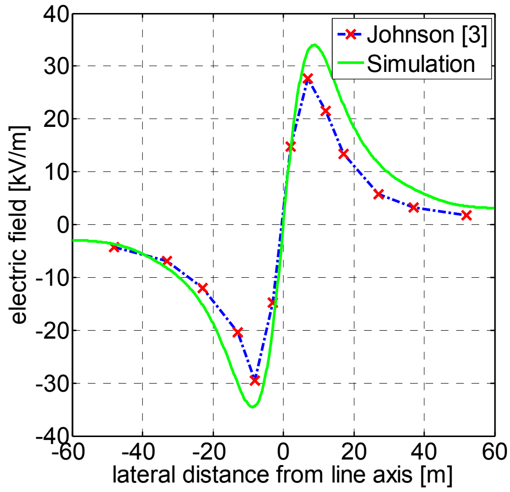

Figure 6: Foul weather (rain) electric field under the line

4.3 Ion Current onto Ground

The resulting ion currents onto ground are depicted in Figure 7 and Figure 8 for fair and foul weather respectively.

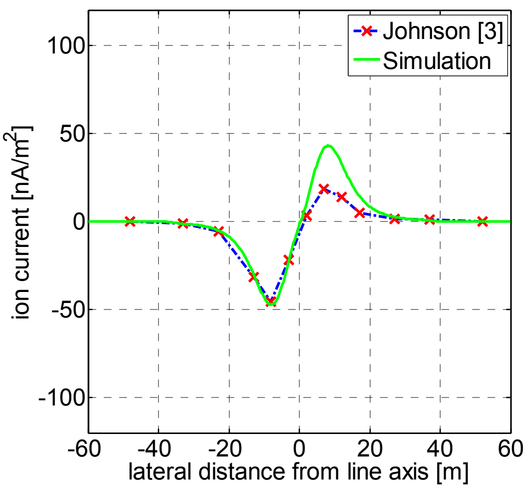

Figure 7: Fair weather ion current under the line

While the negative values between measurement and calculation coincide fairly well, the positive values differ relevantly.

The reason for this is that the measurement shows a similar behaviour as for the electric fields presented above, while the calculations do not. During fair and foul weather the measured asymmetry is large and small, respectively. The contrary is the case for the calculation, where the asymmetry is largest during foul weather conditions, with, especially noticeably, larger currents below the negative than the positive pole. As the only difference between the polarities in the foul weather simulation is given by the mobilities, the latter must be responsible for this behaviour.

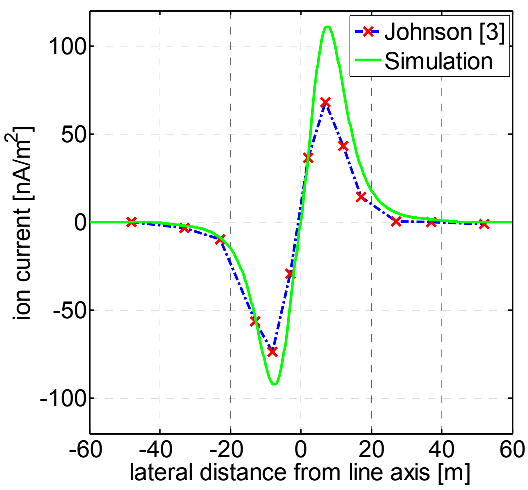

Figure 8: Foul weather (rain) ion current under the line

5 DISCUSSION

In both weather situations, the calculated electric fields on and ion currents onto ground are larger than the measured ones.

The largest differences between measurement and calculation occur in the ion currents of negative ions (right side from the line axis in Figure 7 and Figure 8). As to the foul weather calculation parameters only the mobilities are different, the calculated asymmetry would be reduced when choosing mobilities with smaller difference between the values for positive and negative ions.

The remaining calculation results match the experimental data fairly well. Still improvement of stabilisation techniques, as advocated by [9], seems desirable, improved matching of measured and calculated data seems to be primarily possible by a more appropriate choice of boundary conditions.

6 CONCLUSION

- The example calculations of the time-dependently formulated ion flow field problem shows promising results.
- Improvement of the calculation results seems to be possible by better choices of boundary conditions rather than better stabilisation techniques.
- This method can be applied to investigate time-dependent ion flow fields, such as dampening of transient overvoltages by corona. The authors plan to adopt the method for hybrid lines with AC and DC transmission on one tower or corridor.

7 ACKNOWLEDGMENTS

The English corrections of B. Straumann on this paper are acknowledged gratefully.

8 REFERENCES

[1] L.D. Anzivino, G. Gela, W.W. Guidi, G.B. Johnson, J.J. LaForest, C.W. Nicholls, H.M. Schneider, L. E. Zaffanella, "HVDC Transmission Line Reference Book", Electric Power Research Institute, 3412 Hillview Avenue, Palo Alto, California, 1993.

[2] T. D. Bracken, A. S. Capon, D. V. Montgomery, "Ground Level Electric Fields and Ion Currents on the Celilo-Sylmar ±400 kV DC Intertie During Fair Weather", Vol. 97, No. 2, pp. 370-378, 1978

[3] G. B. Johnson, "Electric Fields and Ion Currents of a ±400 kV HVDC Test Line", IEEE Trans. Power Appar. Syst., Vol. 102, No. 8, pp. 2559-2568, 1983

[4] T. Takuma, T. Ikeda, T. Kawamoto, „Calculation of Ion Flow Fields of HVDC Transmission Lines by the Finite Element Method“, Trans. Power Appar. Syst., Vol. 100, No. 12, pp. 4802-4810, 1981

[5] W. Janischewskyj, G. Cela, "Finite Element Solution for Electric Fields of Coronating DC Transmission Lines", Trans. Power Appar. Syst., Vol. 98, No. 3, pp. 1000-1012, 1979

[6] B.L. Qin, J.N. Sheng, Z. Yan, G. Gela, "Accurate Calculation of Ion Flow Field Under HVDC Bipolar Transmission Lines", IEEE Trans. Power Del., Vol. 3, No. 1, pp. 368-376, 1988

[7] T. Lu, H. Feng, Z. Zhao, X. Cui, "Analysis of the Electric Field and Ion Current Density Under Ultra High-Voltage Direct-Current Transmission Lines Based on Finite Element Method", IEEE Trans. Magn., Vol. 43, No. 4, pp. 1221-1224, 2007

[8] W. Li, B. Zhang, J. He, R. Zeng, S. Chen, „Research on Calculation Method of Ion Flow Field under Multi-circuit HVDC Transmission Lines“, Proc. 20th Int. Zurich Symposium on EMC, Zurich, Switzerland, pp. 133-136, 2009

[9] J. Liu, J. Zou, J. Tian, J. Yuan, "Analysis of Electric Field, Ion Flow Density, and Corona Loss of Same-Tower Double-Circuit HVDC Lines Using Improved FEM", IEEE Trans. Power Del., Vol. 24, No. 1, pp. 482-483, 2009

[10] M. Abdel-Salam, Z. Al-Hamouz, "A Finite-Element Analysis of Bipolar Ionized Field", IEEE Trans. Ind. Appl., Vol. 31, No. 3, pp. 477-483, 1995

[11] B. Zhang, J. He, R. Zeng, S. Gu, L. Cao, "Calculation of Ion Flow Field Under HVdc Bipolar Transmission Lines by Integral Equation Method", IEEE Trans. Magn., Vol. 43, No. 4, pp. 1237-1240, 2007